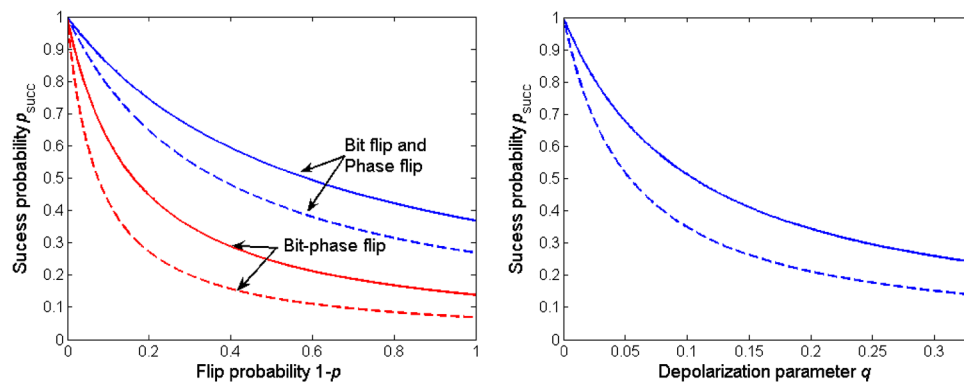


Realization of Single-Photon Frequency-Domain Qubit Channels Using Phase Modulators

Volume 4, Number 6, December 2012

José Capmany
Carlos R. Fernández-Pousa



DOI: 10.1109/JPHOT.2012.2226022
1943-0655/\$31.00 ©2012 IEEE

Realization of Single-Photon Frequency-Domain Qubit Channels Using Phase Modulators

José Capmany¹ and Carlos R. Fernández-Pousa²

¹ITEAM Research Institute, Universidad Politécnica de Valencia, 46022 Valencia, Spain

²Department of Communications Engineering, Universidad Miguel Hernández, 03202 Elche, Spain

DOI: 10.1109/JPHOT.2012.2226022
1943-0655/\$31.00 ©2012 IEEE

Manuscript received July 19, 2012; revised October 14, 2012; accepted October 16, 2012. Date of publication October 22, 2012; date of current version November 13, 2012. This paper was supported in part by the Ministerio de Economía y Competitividad, Spain, through Projects TEC2011-29120-C05-02 and 05 and in part by the Generalitat Valenciana through the PROMETEO 2008/092 research excellence award. Corresponding author: C. R. Fernández-Pousa (e-mail: c.pousa@umh.es).

Abstract: In a recent paper, [4] have developed a scheme for the stochastic implementation of arbitrary quantum operations on multimode single-photon qudit states by using reconfigurable linear-optic systems. Based on this idea, we explore the use of phase modulation for the realization of qubit channels in the frequency basis. Single-photon states belonging to two different frequency modes differing by the modulator's driving frequency represent the input dual-rail qubit states. The channel is implemented by a phase modulator followed by a fiber Bragg grating, taking advantage of the high degree of reconfigurability and microwave bandwidth shown by electrooptic modulation technology. The channels are realized by a combination of three techniques: 1) suitably designed driving waveforms, which are probabilistically addressed to the modulator; 2) the corresponding addressing probabilities; and 3) the grating transmittance at the values of the frequency basis. The proposed scheme results in nonoptimal success probabilities but is shown to allow for a compact implementation of the conventional qubit random unitary channels and the qubit amplitude-damping channel.

Index Terms: Quantum information, microwave photonics.

1. Introduction

Identifying and developing versatile technological platforms and key experimental resources for the practical implementation of quantum processing systems are critical demands in quantum information science [1]. Quantum optics is one of the technical alternatives [2], which takes advantage not only on the recent progress on compact single-photon generation and detection but also on the ability to filter, couple, and route radiation modes using conventional guided-wave technology.

One of the hallmarks of photonic quantum processing is the possibility of implementing systems nondeterministically using linear optics [3]. In the same spirit, Piani *et al.* have recently developed a scheme for the stochastic implementation of arbitrary quantum operations on multimode qudits [4]. This proposal requires reconfigurable and probabilistically addressed multimode linear-optic networks and is based on the successive implementation of each of the Kraus operators in the operator-sum representation of the quantum channel. The action of a single Kraus operator can be reproduced by a linear system implementing its singular-value decomposition [4]–[6], and thus, a reconfigurable system is required to provide the complete set of operators. Random switching

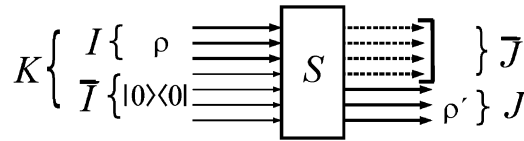


Fig. 1. Scheme of a linear multimode system. The input state ρ is contained in the I modes (thick lines), whereas the modes \bar{I} are in the vacuum state (thin lines). After the interaction output modes \bar{J} are filtered (dotted lines followed by a box) and ρ' is the reduced output state.

among the different systems' configurations then stochastically reproduces the channel if the probabilities of addressing each system's setting follow a certain design condition, as described in [4]. Fischer *et al.* [7] have used this idea to demonstrate optimal single-qubit damping channels in polarization basis, attaining the optimal success probability calculated in [4] and surpassing the success probability of an alternative construction [8], [9].

The use of the two key resources, i.e., linear-systems reconfigurability and randomness in addressing, may impose, however, stringent demands from the experimental point of view depending on the channel under consideration, qudit dimensionality, and the type of mode profiles defining the qudits. Once a mode basis has been chosen, it is natural to consider the level of reconfigurability of the associated linear systems. In [7], for instance, the switching between Kraus operators in polarization basis has been performed by use of liquid-crystal retarders at a rate of 10 Hz. In this regard, the use of the frequency degree of freedom of the optical radiation offers the possibility of employing standard telecom, highly reconfigurable hardware, to implement at quantum level procedures involving linear-optic networks. Frequency modes have been used as the natural basis for frequency-coded quantum key distribution [10], [11] and its SCM/WDM generalizations [12] at addressing rates in the MHz range, and can also be used to reproduce standard quantum-optical effects such as two-photon interference [13], [14].

In a recent paper [15], we have shown how phase modulators (PMs) can be operated to conditionally implement qubit unitaries in dual-rail frequency basis. This basis is associated to single-photon wavepackets of two central frequencies ω_0 and ω_1 defining the encoding set and is used together with fiber Bragg gratings (FBGs) for performing filtering and routing tasks. In this paper, we show that three basic functionalities of conventional PM and FBG technology can be used to meet the practical demands of the construction in [4], specifically, the design of modulator's driving waveforms to tailor the coupling between different frequency modes, the addressing probabilities used to sequentially operate the modulator, synchronously with the input state generation rate, and the design of grating transmittance at the values of the frequency basis. The overall success probabilities of the implementations presented here are in fact lower than the theoretical optimum derived in [4] but exemplify, as in [13] and [14], the potential of low-cost FBG and electrooptic modulation technologies for the implementation of quantum processing tasks.

This paper is organized as follows: In Section 2, we briefly introduce the formalism describing conditional linear-optic quantum operation on single photons, which is the basis for the construction of Piani *et al.* [4] reviewed in Section 3. Here, we also study nonoptimal implementations of this construction in terms of success probabilities. In Section 4, we sketch the construction of dual-rail frequency-encoded qubit unitaries presented in [15], which is used to explore the success probability of random unitary channels in Section 5. Finally and using the same techniques as in [15], we present in Section 6 the conditional realization of the archetypal nonunitary qubit channel, the amplitude-damping channel, and end in Section 7 with our conclusions.

2. Conditional Single-Photon Linear Quantum Operations

Let us consider, as depicted in Fig. 1, an input quantum system composed of K bosonic modes. This mode set is decomposed in two subsets $K = I \cup \bar{I}$ associated to the product Hilbert space $\mathcal{H}_K = \mathcal{H}_I \otimes \mathcal{H}_{\bar{I}}$. Input states ρ are entirely contained in the first set of modes I , whereas the complementary set \bar{I} describes an ancillary space in the vacuum state $|0\rangle\langle 0|$. The total input $\rho \otimes |0\rangle\langle 0|$

undergoes a unitary evolution S and is subsequently reduced to mode set J ($K = J \cup \bar{J}$) leading to an output ρ'

$$\rho \rightarrow \rho' = \text{tr}_{\bar{J}}[S(\rho \otimes |0\rangle\langle 0|)S^\dagger]. \quad (1)$$

We assume that the dimensions $|I|$ and $|J|$ of the input and output mode sets are finite but not necessarily equal. Additionally, we assume that the input state is composed of a single photon and that the interaction S is linear and therefore preserves the photon number. The restriction of operator S to one-photon states is thus defined over the direct sum of one-photon subspaces attached to each of the K modes. Single-photon input states are of the form $\rho \otimes |0\rangle\langle 0| = \sum_{m,n \in I} \rho_{mn} |1_m\rangle\langle 1_n|$ with $|1_n\rangle = a_n^\dagger |0\rangle$ being the n -mode one-photon state and, after the interaction, $S(\rho \otimes |0\rangle\langle 0|)S^\dagger = \sum_{m,n \in K} \bar{\rho}_{mn} |1_m\rangle\langle 1_n|$. The partial trace in (1) involves both the vacuum state and one-photon states in $\mathcal{H}_{\bar{J}}$ and leads to a trace-preserving quantum operation given by

$$\rho \rightarrow \rho' = (1 - p'_{\text{succ}})|0\rangle\langle 0| + p'_{\text{succ}}\tilde{\rho} \quad (2)$$

where $|0\rangle\langle 0|$ and $\tilde{\rho}$ are now states of \mathcal{H}_J representing the absence of output or the actual exit of the photon in the J modes, respectively, which is explicitly given by

$$\tilde{\rho} = \frac{1}{p'_{\text{succ}}} P_J S(\rho \otimes |0\rangle\langle 0|) S^\dagger P_J = \frac{1}{p'_{\text{succ}}} \sum_{m,n \in J} \bar{\rho}_{mn} |1_m\rangle\langle 1_n|. \quad (3)$$

Here, $P_J = \sum_{n \in J} |1\rangle_n \langle 1| \otimes |0\rangle_{\bar{J}} \langle 0|$ is the projector over the one-photon subspace of modes J and $p'_{\text{succ}} = \text{tr}[P_J S(\rho \otimes |0\rangle\langle 0|) S^\dagger] = \sum_{n \in J} \bar{\rho}_{nn}$ is the success probability of the conditional generation of state $\tilde{\rho}$.

A convenient matrix representation of (2) can be constructed as follows. We define the matrix elements S_{mn} of operator S in the single-photon subspace as $S_{kj} = \langle 1_k | S | 1_j \rangle$ [15] so that, for a pure single-photon pure input state $|\Psi\rangle$ in \mathcal{H}_I

$$P_J S(|\Psi\rangle \otimes |0\rangle_{\bar{J}}) = P_J S\left(\sum_{n \in I} c_n |1_n\rangle\right) = \sum_{m \in J, n \in I} S_{mn} c_n |1_m\rangle \quad (4)$$

and therefore, $\tilde{\rho}$ in (3) is determined by the $|J| \times |I|$ submatrix $L_{mn} = S_{mn}$. In terms of matrix L , (2) can be presented as

$$\rho \rightarrow \rho' = [1 - \text{tr}(L\rho L^+)]|0\rangle\langle 0| + L\rho L^+. \quad (5)$$

Success probabilities $p'_{\text{succ}} = \text{tr}(L\rho L^+)$ depend, in general, on the input state ρ , with a maximum value that depends on the spectral norm of matrix L , $\|L\|_\infty$. The prime in p'_{succ} is to explicitly signal the dependence on the input. Both observations follow after introducing the singular value decomposition of $L: L = VDW^+$ with V and W unitaries and D being a diagonal $|J| \times |I|$ matrix with $N = \min(|I|, |J|)$ singular values $\lambda_1 \geq \lambda_2 \geq \dots \geq \lambda_N \geq 0$. Then

$$p'_{\text{succ}} = \text{tr}(L\rho L^+) = \text{tr}(DW^+\rho W D^+) = \sum_{q=1}^N \lambda_q^2 (W^+\rho W)_{qq} \leq \lambda_1^2 \sum_{q=1}^N (W^+\rho W)_{qq} \quad (6)$$

where we have used that $(W^+\rho W)_{qq} \geq 0$ since ρ is a positive operator. From the expression before the inequality, it is clear that p'_{succ} depends, in general, on the input state ρ through the values of $(W^+\rho W)_{qq}$. Now, from $1 = \text{tr}(\rho) = \text{tr}(W\rho W^+) = \sum_{i=1}^{|I|} (W\rho W^+)_{ii}$ with $|I| \geq N$, it follows that $p'_{\text{succ}} \leq \lambda_1^2$. This bound is reached by pure states in the direction of the right singular vector of L corresponding to the maximum singular value λ_1 , and therefore

$$\max_{\rho} p'_{\text{succ}} = \max_q \left\{ \lambda_q^2 \right\} = \lambda_1^2 = \|L\|_\infty^2 \leq 1. \quad (7)$$

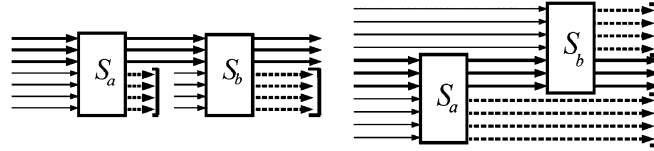


Fig. 2. Schemes of the cascade association of two conditional linear transformations differing in the ancillary spaces of each subsystem. In the right plot, intermediate discarded modes are not reused in the second interaction, and therefore only a unique filtering stage is necessary.

The squared norm $\|L\|_\infty^2 = \lambda_1^2$ is thus the maximum attainable success probability. In (7), $\|L\|_\infty = \max_{|\psi\rangle} \|L|\psi\rangle\| = \lambda_1$ is the spectral norm of matrix L , and the maximum is taken over normalized one-photon states $|\psi\rangle$ in \mathcal{H}_J . The last inequality in (7) follows because the action of unitary S over $|\psi\rangle$ can be decomposed in orthogonal subspaces, $S|\psi\rangle = L|\psi\rangle + L'|\psi\rangle$, where these vectors are one-photon states in \mathcal{H}_J and $\mathcal{H}_{\bar{J}}$, respectively. From this, we get $1 = \|L|\psi\rangle\|^2 + \|L'|\psi\rangle\|^2$, so that $\|L|\psi\rangle\| \leq 1$, and thus, $\|L\|_\infty \leq 1$.

Finally, we briefly describe the cascade association of conditional linear transformations of the form (5) associated to matrices L_a and L_b . Referring to the two configurations in Fig. 2 and noticing that linear systems S_a and S_b leave invariant the vacuum state, it is straightforward to show that both schemes lead to a transformation of the form (5), where, now, $L = L_b L_a$, so that the cascade association implies matrix multiplication with $\rho'_{\text{succ},ba} = \text{tr}(L\rho L^+) = \text{tr}(L_b L_a \rho L_a^+ L_b^+)$.

3. Random Conditional Realization of Qudit Quantum Channels

In this section, we introduce the construction of quantum channels for qudit states ρ proposed by Piani *et al.* [4]. Given a quantum operation in a certain Kraus form

$$\rho \rightarrow \rho' = \sum_n A_n \rho A_n^+ \quad \sum_n A_n^+ A_n = 1 \quad (8)$$

the objective is to construct a conditional realization of this channel of the form

$$\rho \rightarrow \rho' = (1 - p_{\text{succ}})|0\rangle\langle 0| + p_{\text{succ}} \sum_n A_n \rho A_n^+ \quad (9)$$

for a certain success probability $0 < p_{\text{succ}} \leq 1$ independent of the input state ρ , in contrast to general linear one-photon transformations of the form (2). Equation (9) can be interpreted as the result of passing the deterministic channel (8) through a beamsplitter with transmittance p_{succ} in every output mode and subsequently reducing the output to J modes.

The proposal in [4] provides a realization based on probabilistic switching between conditional linear transformations of the form (5). A certain reconfigurable linear system sequentially commutes between different L_n values, which are chosen to be proportional to Kraus operators A_n ($L_n \propto A_n$) and randomly operated with probabilities p_n ($\sum_n p_n = 1$). Then, each time the linear system is addressed, it conditionally realizes a single Kraus operator. The channel implemented this way is

$$\rho \rightarrow \rho' = \left(1 - \sum_n p_n \text{tr}(L_n \rho L_n^+)\right) |0\rangle\langle 0| + \sum_n p_n L_n \rho L_n^+ \quad (10)$$

where $\text{tr}(L_n \rho L_n^+)$ is the success probability of the conditional realization of the (unnormalized) state $L_n \rho L_n^+$. This success probability, in general, depends on the input ρ as analyzed in Section 2. However, if probabilities p_n are found such that

$$\sqrt{p_n} L_n = \eta e^{i\alpha_n} A_n \quad (11)$$

for arbitrary phases α_n and a common constant $0 < \eta \leq 1$, it is immediate to show that (10) provides a conditional realization of (8) of the form (9) with $\rho_{\text{succ}} = \eta^2$ independent of input state ρ .

The paper by Piani *et al.* [4] is mainly concerned with the optimal realization of this construction, i.e., with the proper choice of the set of Kraus operators $\{A_n\}$ and addressing probabilities p_n for maximizing the success probability ρ_{succ} . They first showed that the maximal ρ_{succ} associated to a given set $\{A_n\}$ is

$$\rho_{\text{succ}}(\{A_n\}) = \frac{1}{\sum_n \|A_n\|_\infty^2} \quad (12)$$

which is reached with operators L_n with $\|L_n\|_\infty = 1$ and addressing probabilities $p_q = \|A_q\|_\infty^2 / \sum_n \|A_n\|_\infty^2$ (*Theorem 1* in [4]). From our characterization in (7), condition $\|L_n\|_\infty = 1$ implies that, for all operators L_n , there exist at least one input state (which can be different for each n) for which the success probability of the n -addressing is maximal. Subsequently, they studied the optimization $\rho_{\text{succ,opt}} = \max_{\{A_n\}} \rho_{\text{succ}}(\{A_n\})$ over different sets of Kraus operators $\{A_n\}$ by using entanglement measures.

In summary, once the optimal set of Kraus operators $\{A_n\}$ are determined, it is required a reconfigurable linear-optic device to realize, perhaps conditionally, and address probabilistically a collection of operators $L_n \propto A_n$ with $\|L_n\|_\infty = 1$. As noticed in the introduction, these requirements may be experimentally challenging, so it is natural to pose the problem in a weaker form, i.e., searching for suboptimal realizations associated to operators $L_n \propto A_n$ with $\|L_n\|_\infty \leq 1$. In this regard, there are two practical observations that are worth analyzing.

First, given an n -reconfigurable linear system with $L_n \propto A_n$ where, in general, $\|L_n\|_\infty \leq 1$, the proportionality can be always resolved as (11), i.e., there exist addressing probabilities p_q ($\sum_q p_q = 1$) and a common constant $0 < \eta \leq 1$ ($\rho_{\text{succ}} = \eta^2$) verifying (11). As for the addressing probabilities, the solution is simply

$$p_q = \frac{\|A_q\|_\infty^2 / \|L_q\|_\infty^2}{\sum_n \|A_n\|_\infty^2 / \|L_n\|_\infty^2} \quad (13)$$

and from this, since (11) implies $p_n \|L_n\|_\infty^2 = \rho_{\text{succ}} \|A_n\|_\infty^2$, the success probability must be given by

$$\frac{1}{\rho_{\text{succ}}} = \sum_n \frac{\|A_n\|_\infty^2}{\|L_n\|_\infty^2}. \quad (14)$$

To show finally that $\rho_{\text{succ}} \leq 1$, we use a bound based on the triangle inequality (cf. *Observation 1* in [4])

$$\sum_n \frac{\|A_n\|_\infty^2}{\|L_n\|_\infty^2} \geq \sum_n \|A_n\|_\infty^2 = \sum_n \|A_n^+ A_n\|_\infty \geq \left\| \sum_n A_n^+ A_n \right\|_\infty = \|1\|_\infty = 1 \quad (15)$$

where we have used $\|L_n\|_\infty \leq 1$ and (8). Therefore, proportionality $L_n \propto A_n$ is sufficient to construct a conditional but, in general, nonoptimal realization of the channel. Note that, since $\|L_n\|_\infty \leq 1$, ρ_{succ} in (14) is maximized by operators $\|L_n\|_\infty = 1$ and given by (12); this is the content of *Theorem 1* in [4].

The second observation is that it is possible to construct a simple bound for the departure of ρ_{succ} from the optimal value $\rho_{\text{succ}}(\{A_n\})$ in terms of the departure of $\|L_n\|_\infty$ from 1. First, from (13)–(15), we get

$$\frac{\rho_{\text{succ}}}{\rho_{\text{succ}}(\{A_n\})} = \sum_n p_n \|L_n\|_\infty^2 \quad (16)$$

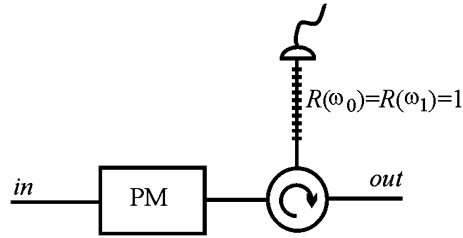


Fig. 3. Circuit layout for the conditional implementation of 2×2 linear transformations.

and from $\min_n \|L_n\|_\infty \leq \|L_n\|_\infty \leq \max_n \|L_n\|_\infty$, we obtain

$$\min_n \|L_n\|_\infty^2 \leq \frac{P_{\text{succ}}}{P_{\text{succ}}(\{A_n\})} \leq \max_n \|L_n\|_\infty^2 \quad (17)$$

which shows that the relative success probability is not higher (resp., lower) than the higher (resp., lower) maximal success probability associated to the conditional realization of each Kraus operator.

4. Conditional Frequency-Encoded Qubit Linear Operations

The construction of conditional qubit unitaries in [15] is based on the use of both PM and FBG to mix and filter single-photon wavepackets at two central frequencies ω_0 and ω_1 , which define the dual-rail basis for qubit representation. From the classical point of view, PM can be described as a transformation of the optical envelope at central frequency ω given by

$$A(t)\exp(-i\omega t) \rightarrow A(t)\exp[-i\omega t - ix(t)] = A(t) \sum_{k=-\infty}^{\infty} C_k \exp(-i\omega t - ik\Omega t) \quad (18)$$

where we have assumed that the modulation function $x(t)$ is periodic with angular frequency Ω in the microwave range, as is the usual driving regime of PM, and C_k are the corresponding Fourier coefficients. From the quantum point of view [16], single-photon wavepackets at a certain central optical frequency ω_0 undergo shifts in frequency by $k\Omega$, C_k being the probability amplitude for such a process of sideband generation. To be amenable to manipulation, photons are to be organized in frequency channels, i.e., the spectral spread $\Delta\omega$ of single-photon wavepackets is to be lower than Ω .

Frequency-encoded dual-rail qubits are defined by referring to a basis composed of single photons at an optical frequency ω_0 and at its first sideband, $\omega_1 = \omega_0 + \Omega$, which is the most favorable situation in terms of probability amplitudes [15]. As described in this reference, current commercial electrooptic modulators feature bandwidths up to several tens of GHz, and therefore, Ω may lie in the microwave or mm-wave range. According to the observation in the previous paragraph, this requires photon wavepackets of duration $1/\Delta\omega$ of the order of nanoseconds. The basic setup for the conditional implementation of frequency-encoded qubit linear operations is depicted in Fig. 3 and uses standard modulation and filtering techniques from microwave photonics. The spectral filtering is performed by a FBG with total reflectivity at frequencies ω_0 and ω_1 , so that a detector at the transmission FBG end fires when the photon exits the encoding set $\{\omega_0, \omega_1\}$. The circulator directs the backreflected waves to the physical out port. This setup implements operators of the form

$$L = \begin{bmatrix} C_0 & C_1 \\ C_{-1} & C_0 \end{bmatrix} \quad (19)$$

which can be tailored by an appropriate choice of $x(t)$. In [15], it was shown that the use of simple driving voltages such as single-tone $x(t) = \mu \sin(\Omega t + \theta)$, with μ is the modulation index, or two-tone

in the triple frequency $x(t) = \mu_1 \sin(\Omega t + \theta) + \mu_3 \sin(3\Omega t + 3\theta)$ lead to a family of qubit unitaries of the form

$$L = \sqrt{\rho_{\text{succ}}} \begin{bmatrix} \sqrt{1-\kappa} & e^{i\theta} \sqrt{\kappa} \\ -e^{-i\theta} \sqrt{\kappa} & \sqrt{1-\kappa} \end{bmatrix}. \quad (20)$$

For single-tone modulation, the probability amplitudes in the Fourier expansion (18) are given by $C_k = e^{i\theta k} J_k(\mu)$, J_k being the Bessel function of first kind and order k . The corresponding success probabilities and coupling constants are

$$\rho_{\text{succ}} = J_0(\mu)^2 + J_1(\mu)^2 \quad \kappa = \frac{J_1(\mu)^2}{J_0(\mu)^2 + J_1(\mu)^2}. \quad (21)$$

In particular, the success probabilities associated to the realization of the standard basis $\{\sigma_k, k = 0, \dots, 3\}$, where σ_0 is the identity matrix and σ_k ($k = 1, 2, 3$) are the Pauli matrices, can be computed as follows. Under single-tone modulation, $(st)\sigma_0$ is realized in form (20) with a null driving voltage $\mu = 0$, which implies $\kappa = 0$. For $\mu = 2.44$ ($\kappa = 1$), we can proportionally realize the first two Pauli matrices σ_1 and σ_2 by adjusting the driving phase θ , $L(\kappa = 1, \theta = 0) \equiv L_{\sigma_1} \propto \sigma_1$, and $L(\kappa = 1, \theta = \pi/2) \equiv L_{\sigma_2} \propto \sigma_2$. The maximal success probabilities are

$$\rho_{\text{succ}}(\sigma_0, st) = \|L_{\sigma_0}\|_{\infty}^2 = 1, \quad \rho_{\text{succ}}(\sigma_1, st) = \|L_{\sigma_1}\|_{\infty}^2 = \rho_{\text{succ}}(\sigma_2, st) = \|L_{\sigma_2}\|_{\infty}^2 = 0.27. \quad (22)$$

Finally, we obtain σ_3 as the cascade $\sigma_3 = -i\sigma_1\sigma_2$, resulting in

$$\rho_{\text{succ}}(\sigma_3, st) = \|-iL_{\sigma_1}L_{\sigma_2}\|_{\infty}^2 = \|L_{\sigma_1}\|_{\infty}^2 \|L_{\sigma_2}\|_{\infty}^2 = 0.27^2 = 0.07. \quad (23)$$

These success probabilities can be increased in two-tone (tt) modulation by optimizing the modulation indices μ_1 and μ_3 [15]. In the case of the Pauli basis

$$\rho_{\text{succ}}(\sigma_0) = 1, \quad \rho_{\text{succ}}(\sigma_1, tt) = \rho_{\text{succ}}(\sigma_2, tt) = 0.37, \quad \rho_{\text{succ}}(\sigma_3, tt) = 0.37^2 = 0.14. \quad (24)$$

With these values and (14), it is immediate to explore the success probabilities that can be reached with PM for qubit random unitary channels, as will be done in the next section. However, it is clear that the construction of conditional qubit linear operators is not exhausted by unitaries, as the matrix (19) can be tailored by more complex driving voltages. The construction of the amplitude damping channel below provides an example of this general approach.

5. Realization of Random Unitary Qubit Channels

As a first application we explore the attainable success probability of the conditional realization of random unitary qubit channels using PM. These channels are defined as convex combinations of unitary transformations, which, in the case of qubits, can be presented as

$$\rho \rightarrow \rho' = \sum_{n=0}^3 q_n \sigma_n \rho \sigma_n \quad \sum_n q_n = 1. \quad (25)$$

The standard bit, phase, and bit-flip channels, together with the depolarizing channel, belong to this category [1]. For the first three channels, the standard parametrization involves two nonnull q_n in the sum (25): $q_0 = p$ is common to the three channels, the other being $q_1 = 1 - p$ for bit, $q_2 = 1 - p$ for phase, and $q_3 = 1 - p$ for bit-phase flip, where $1 - p$ stands for the corresponding flip probability. The depolarizing channel, in turn, involves the four matrices with $q_1 = q_2 = q_3 \equiv q$ and $q_0 = 1 - 3q$ ($0 \leq q \leq 1/3$). In either case, the Kraus operators in (25) are $A_n = \sqrt{q_n} \sigma_n$, and the optimal success probability given by (12) is unity.

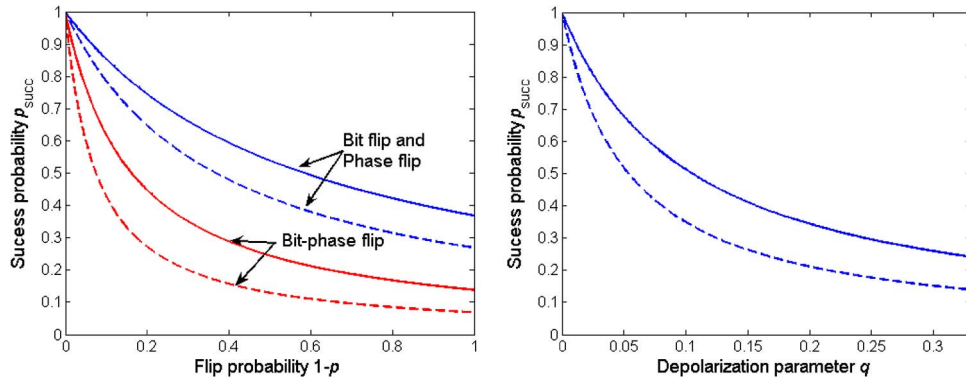


Fig. 4. (Left, blue) Success probabilities of bit flip and phase flip channels, (left, red) bit–phase flip channel, and (right) the depolarizing channels using phase modulation. In each case, dotted curves correspond to single-tone modulation and continuous curves to two-tone modulation.

With nonoptimal operators $L_n \propto A_n$ with $\|L_n\|_\infty^2 \leq 1$, of course, the success probability is lower. For bit, phase, and phase-flip channels, equation (14) yields

$$\frac{1}{p_{\text{succ}}} = \sum_n \frac{q_n}{\|L_{\sigma_n}\|_\infty^2} = p + \frac{1-p}{\|L_{\sigma_k}\|_\infty^2} \quad (26)$$

where $\|L_{\sigma_k}\|_\infty^2$ represents the success probability of the realization of Pauli unitary σ_k ($k = 1, 2, 3$) as given by (22) and (23) in single-tone modulation or by (24) in two-tone modulation. For the depolarizing channel, we obtain

$$\frac{1}{p_{\text{succ}}} = \sum_n \frac{q_n}{\|L_{\sigma_n}\|_\infty^2} = 1 - 3q + q \left(\frac{1}{\|L_{\sigma_1}\|_\infty^2} + \frac{1}{\|L_{\sigma_2}\|_\infty^2} + \frac{1}{\|L_{\sigma_3}\|_\infty^2} \right). \quad (27)$$

The resulting success probabilities are depicted in Fig. 4. It is observed that p_{succ} decreases as the corresponding flip probability $1-p$ or depolarization parameter q increases, as the construction demands a higher addressing rate of Pauli matrices $\{\sigma_1, \sigma_2, \sigma_3\}$ with suboptimal values $\|L_{\sigma_n}\|_\infty^2 < 1$. The upper bound in (17) is equal to 1 and is attained in these curves for $p = 1$ and $q = 0$. The lower bound is reached in the left plot in Fig. 4 for $p = 0$. In turn, the minimum value for the depolarizing channel ($q = 1/3$) is $p_{\text{succ}} = 0.14$ for single-tone modulation and $p_{\text{succ}} = 0.24$ for two-tone modulation. In this case, the lower bound in (17) is not reached because this bound involves a single Kraus operator, the one having the lower success probability of generation.

6. Realization of the Amplitude Damping Channel

The amplitude damping qubit channel is described by the following set of Kraus operators:

$$A_0 = \begin{bmatrix} 0 & \sqrt{\gamma} \\ 0 & 0 \end{bmatrix} \quad A_1 = \begin{bmatrix} 1 & 0 \\ 0 & \sqrt{1-\gamma} \end{bmatrix} \quad (28)$$

where γ is the damping parameter. From (12), the optimal success probability is

$$p_{\text{succ}}(\{A_n\}) = \frac{1}{\gamma + 1} \quad (29)$$

and it can be shown that this success probability is also optimal among all possible set of Kraus operators representing the channel [4].

The proposed realization is based on two modes at frequencies ω_G and ω_E representing the ground and excited states (GS/ES) of a two-level system. We modify the scheme in Fig. 3, where, now, the FBG shows total reflectivity at the GS frequency ω_G , $R(\omega_G) = 1$, and partial reflectivity

$1 - \gamma$ at the ES frequency ω_E , $R(\omega_E) = 1 - \gamma$. The PM will be used to couple these frequencies, so we set $\omega_G = \omega_E + \Omega$, i.e., the GS frequency is represented by the first sideband of the ES frequency. The FBG thus provides two functionalities: first, to filter all frequencies but the dual-rail encoding set $\{\omega_G, \omega_E\}$ and, second, to selectively attenuate the ES mode with respect to the GS mode. The damping parameter γ can be tuned by standard FBG technology, and in basis $\{\omega_G, \omega_E\}$, the action of the FBG is simply given by

$$L_{\text{FBG}} = \begin{bmatrix} 1 & 0 \\ 0 & \sqrt{1-\gamma} \end{bmatrix} \quad (30)$$

which coincides with Kraus operator A_1 in (28).

The possibility of random commutation between the two operators in (30) is provided by two settings in the PM, $L_{\text{PM},0}$, and $L_{\text{PM},1}$. For $L_{\text{PM},1}$, we set a null driving voltage in the modulator, so that the PM action is trivial, $L_{\text{PM},1} = 1$. The action of the PM + FBG cascade is $L_1 = L_{\text{FBG}}L_{\text{PM},1} = A_1$, so the second Kraus operator (30) is realized with $\|L_1\|_\infty = 1$.

On the other hand, comparison of A_0 in (28) with (19) suggest designing a driving PM waveform $x(t)$ yielding $C_0 = C_{-1} = 0$ and $C_1 \neq 0$. The existence of a simple two-tone periodic waveform producing these couplings can be justified as follows. From (20), we observe that the use of a single modulating tone can realize 2×2 antidiagonal operators with equal magnitude in its components and adjustable relative phase. Denoting this single tone as $x_1(t) = \mu_1 \sin(\Omega t + \theta_1)$, this setting corresponds to $\kappa = 1$ or to a modulation index $\mu_1 = 2.404$, which is the index that nullifies $C_0 = J_0(\mu_1)$. In fact, the realization of Pauli matrices σ_1 and σ_2 in Section 4 are based on this setting. Let us arbitrarily choose $\theta_1 = \pi/2$. Using $C_n = \exp(i\theta_1 n) J_n(\mu_1)$, it is immediate to observe that this choice forces $\pm n$ sidebands to be in phase since $J_{-n}(\mu_1) = (-1)^n J_n(\mu_1)$. Then, the modulation impinged by this single tone is

$$A(t) \exp[-i\omega t - ix_1(t)] = A(t) \left[iJ_1(\mu_1) \left(e^{-i(\omega-\Omega)t} + e^{-i(\omega+\Omega)t} \right) - J_2(\mu_1) \left(e^{-i(\omega-2\Omega)t} + e^{-i(\omega+2\Omega)t} \right) + \dots \right] \quad (31)$$

where the dots stand for higher order sidebands. Now, let us design a second single-tone driving voltage $x_2(t) = \mu_2 \sin(2\Omega t + \theta_2)$ at double frequency. In this case, we set $\mu_2 = 1.126$, which corresponds to a transformation with $\kappa = 0.5$ for which $J_0(\mu_2) = J_1(\mu_2)$. We also set $\theta_2 = 0$, so $C_0 = C_1 = -C_{-1}$, i.e., the $+1$ sideband at double frequency is in phase with the carrier and the -1 sideband is in opposition. Then

$$A(t) \exp[-i\omega t - ix_2(t)] = J_0(\mu_2) A(t) \left[e^{-i\omega t} + e^{-i(\omega+2\Omega)t} - e^{-i(\omega-2\Omega)t} + \dots \right]. \quad (32)$$

Now, if we compose these two modulations, i.e., $x(t) = x_1(t) + x_2(t)$, we obtain

$$\begin{aligned} \tilde{A}(t) &= A(t) \exp[-i\omega t - ix_1(t) - ix_2(t)] \\ &= A(t) J_0(\mu_2) \left[2iJ_1(\mu_1) e^{-i(\omega+\Omega)t} - J_2(\mu_1) \left(e^{-i(\omega+2\Omega)t} + e^{-i(\omega-2\Omega)t} \right) + \dots \right] \end{aligned} \quad (33)$$

thus yielding the desired coupling. Of course, this argument is not exact but shows that a good guess for an optimization seed of a driving two-tone waveform $x(t)$ is that given by two in-quadrature tones with modulation indices $\mu_1/2\pi = 0.383$ and $\mu_2/2\pi = 0.179$. The result of an optimization forcing $C_0 = C_{-1} = 0$ and maximizing C_1 , obtained with the procedure described in [15], is shown in Fig. 5. The optimal values are $\mu_1/2\pi = 0.391$ and $\mu_2/2\pi = 0.175$, resulting in $|C_1|^2 = 0.46$. This probability can be increased by use of additional tones at $k\Omega$, but this seems increasingly hard from the experimental point of view.

The optimized waveform in Fig. 5, left, shows a strong similarity to a sawtooth profile. This can be explained as follows: as apparent from (33), the modulator $\exp[-ix(t)]$ should ideally operate as a frequency shifter $A(t) \exp(-i\omega t - i\Omega t)$, transforming frequency ω_E into $\omega_G = \omega_E + \Omega$ and forcing ω_G to leave the encoding set $\{\omega_G, \omega_E\}$. A periodic $x(t)$ generating the targeted couplings is thus the

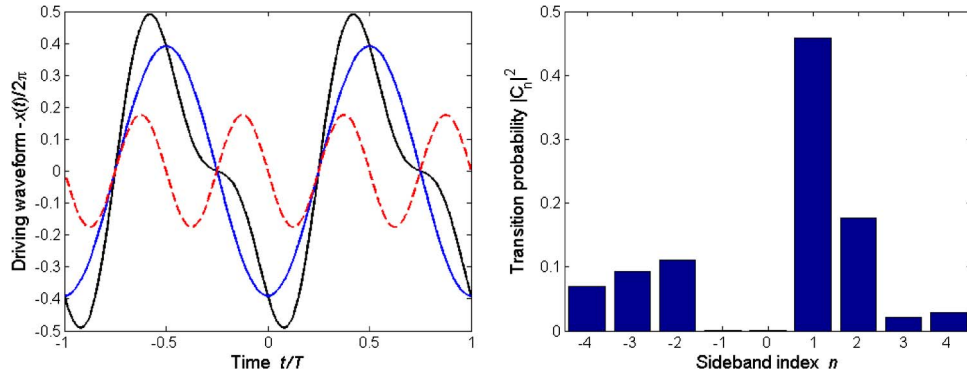


Fig. 5. (Left) Optimized two-tone driving waveform implementing A_0 over two driving periods: blue continuous curve, tone at $\Omega = 2\pi/T$; dashed red curve, tone at 2Ω ; black continuous curve, total waveform. (Right) Transition probabilities $|C_n|^2$ for coupling to sideband n .

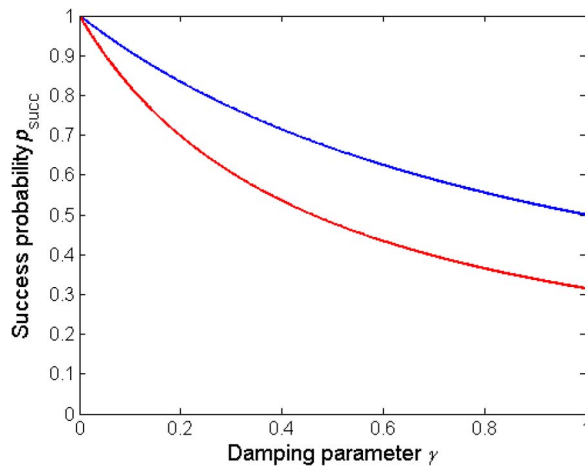


Fig. 6. Success probabilities for the proposed suboptimal realization [red, (36)] and the optimal realization [blue, (29)].

(wrapped) periodization of a linear phase, $-x(t) = -\Omega t = -2\pi t/T$ in the fundamental period $|t| < T/2$, as approximated in Fig. 5 left.

The final matrix describing the PM action is thus

$$L_{PM,0} = e^{i\theta} \sqrt{0.46} \begin{bmatrix} 0 & 1 \\ 0 & 0 \end{bmatrix} \quad (34)$$

and using (30) and (34), the cascade PM + FBG operates as

$$L_0 = L_{FBG} L_{PM,0} = L_{PM,0} \propto A_0 \quad (35)$$

and therefore realizes the first Kraus operator in (28) with $\|L_0\|_\infty^2 = 0.46$. Finally, using (14), we obtain

$$\frac{1}{p_{succ}} = \sum_n \frac{\|A_n\|_\infty^2}{\|L_n\|_\infty^2} = 1 + \frac{\gamma}{0.46}. \quad (36)$$

This success probability is compared with the optimal value (29) in Fig. 6. The suboptimal character of this realization, consequence of norm $\|L_0\|_\infty < 1$, is clearly shown at the minimum value of 0.315 for $\gamma = 1$, as compared with 0.50 of the optimal realization. If we compare (36) with

the alternative realization of the amplitude-damping channel in polarization basis [8], [9], which shows a uniform success probability of 0.50 for any value of γ , we observe that (36) provides an improvement for low or moderate values of the damping parameter, $\gamma < 0.46$.

7. Conclusion

We have explored the conditional realization of single-qubit quantum channels in frequency basis by using current optical phase modulation and FBG technology, adapting a recent proposal by Piani *et al.* [4] for the implementation of arbitrary qudit quantum operations. The use of electrooptical modulation techniques, together with dual-rail qubits based on frequency modes, has been shown to be a practical alternative to meet the demands required by the original proposal. Phase modulators have been used for proportionally realizing each of the Kraus operators in the channel's operator-sum decomposition and have been subsequently stochastically addressed to conditionally implement the full channel structure. The resulting realizations do not reach the optimal bounds found in [4] but allow for implementations of qubit channels and show the versatility of frequency-encoded qubits for the practical implementation of quantum information tasks.

References

- [1] M. A. Nielsen and I. L. Chuang, *Quantum Computation and Quantum Information*. Cambridge, U.K.: Cambridge Univ. Press, 2000.
- [2] T. C. Ralph, "Quantum optical systems for the implementation of quantum information processing," *Rep. Progr. Phys.*, vol. 69, no. 4, pp. 853–898, Apr. 2006.
- [3] E. Knill, R. Laflamme, and G. J. Milburn, "A scheme for efficient quantum computation with linear optics," *Nature*, vol. 409, no. 6816, pp. 46–52, Jan. 2001.
- [4] M. Piani, D. Pitkanen, R. Kaltenbaek, and N. Lütkenhaus, "Linear-optics realization of channels for single-photon multimode qudits," *Phys. Rev. A*, vol. 84, no. 3, pp. 032304-1–032304-11, Sep. 2011.
- [5] B. He, J. A. Bergou, and Z. Wang, "Implementation of quantum operations on single photon qudits," *Phys. Rev. A*, vol. 76, no. 4, pp. 042326-1–042326-4, Oct. 2007.
- [6] K. Kieling, "Linear optics quantum computing—Construction of small networks and asymptotic scaling," Ph.D. dissertation, Imperial College, London, U.K., 2008.
- [7] K. A. G. Fisher, R. Prevedel, R. Kaltenbaek, and K. J. Resch, "Optimal linear optical implementation of a single-qubit damping channel," *New J. Phys.*, vol. 14, p. 033016, Mar. 2012.
- [8] Q. Lin, J. Li, and G.-C. Guo, "Linear optical realization of qubit purification with quantum amplitude damping channel," *Chin. Phys. Lett.*, vol. 24, no. 7, pp. 1809–1812, Jul. 2007.
- [9] J.-C. Lee, Y.-C. Jeong, Y.-S. Kim, and Y.-H. Kim, "Experimental demonstration of decoherence suppression via quantum measurement reversal," *Opt. Exp.*, vol. 19, no. 17, pp. 16 309–16 316, Aug. 2011.
- [10] J.-M. Merolla, Y. Mazurenko, J.-P. Goedgebuer, L. Duraffourg, H. Porte, and W. T. Rhodes, "Quantum cryptographic device using single-photon phase modulation," *Phys. Rev. A*, vol. 60, no. 3, pp. 1899–1905, Sep. 1999.
- [11] M. Bloch, S. W. McLaughlin, J.-M. Merolla, and F. Patois, "Frequency-coded quantum key distribution," *Opt. Lett.*, vol. 32, no. 3, pp. 301–303, Feb. 2007.
- [12] A. Ruiz-Alba, J. Mora, W. Amaya, A. Martinez, V. Garcia-Muñoz, D. Calvo, and J. Capmany, "Microwave photonics parallel quantum key distribution," *IEEE Photon. J.*, vol. 4, no. 3, pp. 931–942, Jun. 2012.
- [13] L. Olislager, J. Cussey, A. T. Nguyen, P. Emplit, S. Massar, J.-M. Merolla, and K. Phan Huy, "Frequency bin entangled photons," *Phys. Rev. A*, vol. 82, no. 1, pp. 013804-1–013804-7, Jul. 2010.
- [14] L. Olislager, I. Mbodji, E. Woodhead, J. Cussey, L. Furfaro, P. Emplit, S. Massar, K. P. Huy, and J.-M. Merolla, "Implementing two-photon interference in the frequency domain with electro-optic phase modulators," *New J. Phys.*, vol. 14, p. 043015, Apr. 2012.
- [15] J. Capmany and C. R. Fernández-Pousa, "Conditional frequency-domain beamsplitters using phase modulators," *IEEE Photon. J.*, vol. 3, no. 5, pp. 954–967, Oct. 2011.
- [16] J. Capmany and C. R. Fernández-Pousa, "Quantum modelling of electro-optic modulators," *Laser Photon. Rev.*, vol. 5, no. 6, pp. 750–772, Nov. 2011.